

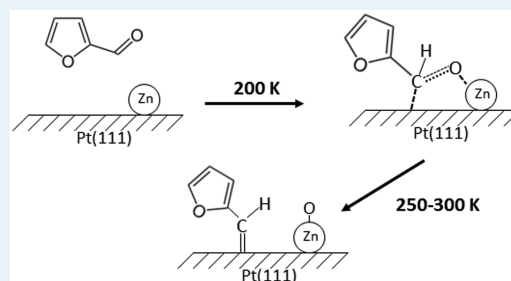
# Deoxygenation of Biomass-Derived Oxygenates: Reaction of Furfural on Zn-Modified Pt(111)

Daming Shi and John M. Vohs\*

Department of Chemical & Biomolecular Engineering, University of Pennsylvania, 220 South 33rd Street, Philadelphia, Pennsylvania 19104-6363, United States

**ABSTRACT:** Temperature-programmed desorption (TPD) and high-resolution electron energy loss spectroscopy (HREELS) were used to characterize the adsorption and reaction of furfural on Pt(111) and Zn-modified Pt(111) surfaces. Furfural was found to bond to Pt(111) via the aromatic ring, which facilitated C–C bond scission and ring opening at low temperatures, leading to unselective decomposition to CO and H<sub>2</sub>. In contrast, on Zn-modified Pt(111), furfural bonds via the aldehyde carbonyl in an  $\eta^2(\text{C},\text{O})$  configuration with the aromatic furan ring tilted away from the surface. This bonding configuration weakens the C–O bond in the carbonyl, which undergoes scission upon heating above 250 K to form a stable (C<sub>4</sub>H<sub>3</sub>O)–CH= intermediate. These results provide useful mechanistic insights for the hydrodeoxygenation of furfural on PtZn catalysts.

**KEYWORDS:** furfural, biomass, re-forming, hydrodeoxygenation, PtZn, Pt(111)



## INTRODUCTION

The desire to produce fuels and chemicals by more sustainable and environmentally sympathetic methods has motivated research on the use of cellulosic biomass as a feedstock.<sup>1–3</sup> The effective utilization of this renewable resource, however, requires the development of efficient chemical pathways and catalysts for the conversion of biomass-derived molecules into more useful products. Due to the high oxygen content in the constituent C<sub>6</sub> and C<sub>5</sub> sugars in cellulose and hemicellulose, at least some deoxygenation is generally required. Hydrodeoxygenation (HDO) of furfurals, which are produced from the dehydration of the sugars, in particular, is a key step in many of the reaction pathways proposed for the upgrading of cellulosic biomass into value-added fuels and chemicals.<sup>4</sup> Traditional metal catalysts that have high hydrogenolysis activity, such as Ni and Pd,<sup>5–7</sup> have been explored for these HDO reactions, but they tend to promote either undesirable decarbonylation that results in a decrease in carbon number or hydrogenation of the aromatic ring.

Several studies in the literature have reported that the decarbonylation activity can be suppressed by alloying a group 10 metal with a second more oxyphilic metal.<sup>8–10</sup> For example, Sitthisa et al.<sup>9</sup> have reported that, for typical HDO conditions, reaction of furfural on supported Ni produces primarily decarbonylation products. Alloying the Ni with Fe, however, dramatically shifts the selectivity to the desired 2-methylfuran HDO product. Another interesting aspect of this study is that hydrogenolysis of the aldehyde carbonyl over Ni–Fe catalysts occurs without hydrogenation or opening of the aromatic furan ring which would be expected on Ni alone.<sup>11</sup> Similar results have also been reported for the HDO of lignin-derived aromatic oxygenates where alloying a group 10 metal with a more

oxyphilic metal (e.g., PtSn, PdZn, and PdFe) enhances HDO selectivity while simultaneously inhibiting the activity for aromatic ring hydrogenation.<sup>12,13</sup>

To provide insight into how alloying alters the activity and selectivity of this class of catalysts, we have recently been studying the reaction of aldehydes and aldoses, including glucose, on model catalysts consisting of Zn-modified Pt(111) and Pd(111) surfaces.<sup>14–16</sup> For the reaction of simple aldehydes, such as acetaldehyde and glycolaldehyde, on Pt(111) it was observed that adding small amounts of Zn to the surface suppressed formation of acyl intermediates which readily undergo decarbonylation and stabilized an  $\eta^2(\text{C},\text{O})$  configuration of the aldehyde carbonyl in which the O is bonded to a Zn site and the C to a Pt site. This bonding configuration results in a weakening of the C–O bond, which facilitates its cleavage.<sup>14</sup> These experimental results are consistent with DFT calculations for similar reactions on Ni and NiFe surfaces reported by Sitthisa et al.<sup>9</sup>

In the work reported here we have expanded our previous temperature-programmed desorption (TPD) and high-resolution electron energy loss spectroscopy (HREELS) studies of the reaction of aldehydes on Zn-modified Pt(111) to include the reaction of furfural on this surface. The goal of the study was to determine how Zn addition to Pt alters the bonding of both the carbonyl and aromatic furan ring to the surface and to identify stable reaction intermediates that are involved in the HDO of furfural on PtZn catalysts.

Received: January 9, 2015

Revised: February 17, 2015

Published: February 25, 2015

## EXPERIMENTAL SECTION

All experiments in this study were conducted in an ultrahigh-vacuum (UHV) apparatus which has been described in previous publications.<sup>14–17</sup> The system was operated with a  $2 \times 10^{-10}$  Torr background pressure, equipped with an SRS RGA200 quadrupole mass spectrometer, an ion sputter gun (PHI electronics), and an HREEL spectrometer (LK Technologies). The Pt(111) single-crystal substrate was 10 mm in diameter and oriented to within  $\pm 0.5^\circ$ . The Pt crystal was spot-welded to two tantalum wires that were connected to a UHV sample manipulator and could be heated resistively and cooled to 115 K by conduction from a liquid N<sub>2</sub> reservoir. The sample was cleaned by repeated cycles of 2 kV Ar<sup>+</sup> ion bombardment at 600 K for 30 min, annealing at 1200 K under vacuum for 15 min, and annealing at 1200 K in  $2 \times 10^{-8}$  Torr O<sub>2</sub> for 15 min.

The furfural reactant (Sigma-Aldrich, 99%) was contained in a glass vial that was attached to a stainless steel manifold connected to the main UHV apparatus via a variable leak valve. A 3 K/s heating rate was used in all TPD experiments. A series of TPD experiments on Pt(111) showed that saturation coverage in the first monolayer occurred for a 0.6 L furfural dose at 115 K. For this reason a 0.6 L furfural dose was used in the TPD experiments reported below.

HREEL spectra were collected using a 4 eV electron beam oriented at  $60^\circ$  with respect to the surface normal. The full width at half-maximum of the elastic peak on the clean surface was typically  $40 \text{ cm}^{-1}$ . HREEL spectra were collected as a function of sample temperature. For temperatures greater than the dosing temperature, the sample was heated at 3 K/s to the indicated temperature and then rapidly quenched to low temperature, at which point the spectrum was collected.

Zn-modified surfaces were prepared by exposing the Pt(111) surface to a beam of Zn atoms produced using a thermal evaporative source that consisted of a small coil of Zn wire (Alfa Aesa, 99.99%) wrapped around a resistively heated tungsten filament. The Zn flux from the source was monitored using a quartz crystal microbalance (QCM), and the total amount of Zn deposited was further quantified by measuring the area of the high-temperature Zn desorption feature in the TPD spectra. Since in each TPD run with a Zn-modified surface the sample was heated to a sufficiently high temperature (1200 K) to cause the Zn to desorb completely, freshly prepared Zn-modified surfaces were used in all of the TPD runs.

The structure of Zn-modified Pt(111) surfaces has previously been reported in detail.<sup>18</sup> In this previous study it was shown that Zn deposition with the Pt(111) sample held at or below room temperature produces Zn adatoms. Annealing between 600 and 700 K causes the adatoms to diffuse into the surface, while heating to higher temperatures induces Zn desorption. For low Zn coverages, the equilibrium structure of the annealed surface is such that the Zn is present in the second and third layers. Thus, in order to provide a model alloy surface that contained both Zn and Pt sites, surfaces with Zn adatoms that were produced at low temperatures were used in this study. Note that, in addition to providing Zn sites on the surface, Zn adatoms also influence the electronic properties and reactivities of nearby surface Pt atoms in a manner similar to that observed for the bulk alloy.

## RESULTS

TPD data obtained following exposure of the clean and Zn-modified Pt(111) surfaces at 115 K to 0.6 L of furfural are displayed in Figures 1–3. As shown by the bottom curve in

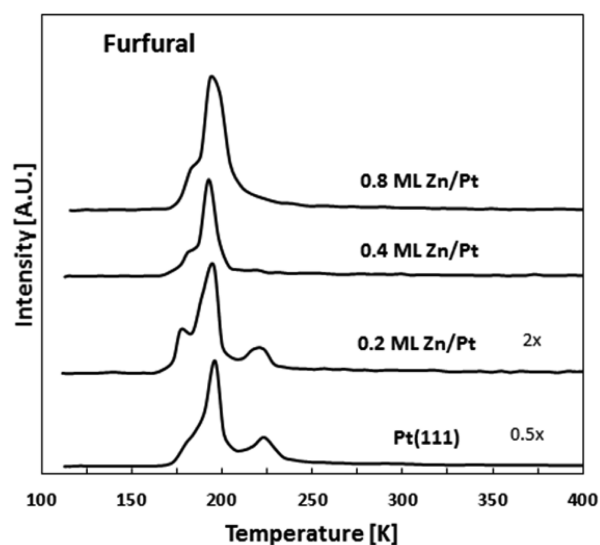


**Figure 1.** Furfural desorption spectra obtained during TPD of Zn-modified Pt(111) surface dosed with 0.6 L of furfural spectra as a function of the Zn coverage.

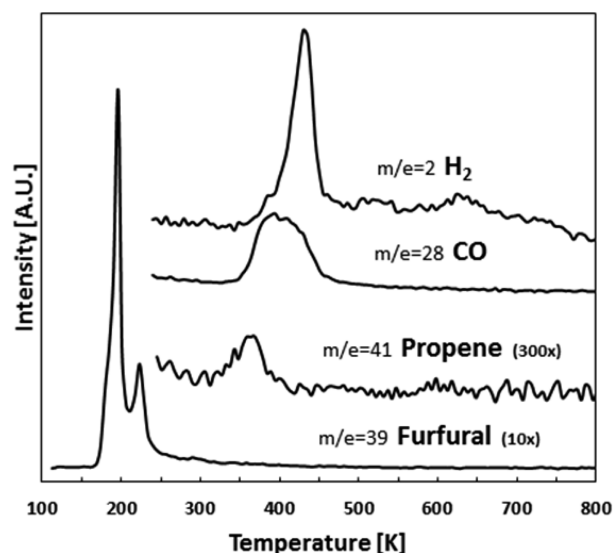


**Figure 2.** TPD spectra obtained following exposure of the Pt(111) surface to 0.6 L of furfural.

Figure 1, for Zn-free Pt(111) weakly adsorbed molecular furfural desorbed in two overlapping peaks centered at 185 and 195 K with an additional peak at 225 K due to a slightly more strongly bonded species. Above 225 K, gaseous reaction products were detected for this surface, with the primary ones being CO and H<sub>2</sub>, as shown in Figure 2. CO desorbed in two overlapping peaks centered at 390 and 415 K, while H<sub>2</sub> desorbed in a large peak at 430 K and a series of much less intense peaks between 500 and 650 K. The CO peaks and the large H<sub>2</sub> peak are both consistent with desorption-limited products,<sup>19</sup> thus demonstrating that adsorbed furfural decomposes at lower temperatures. The only other product detected

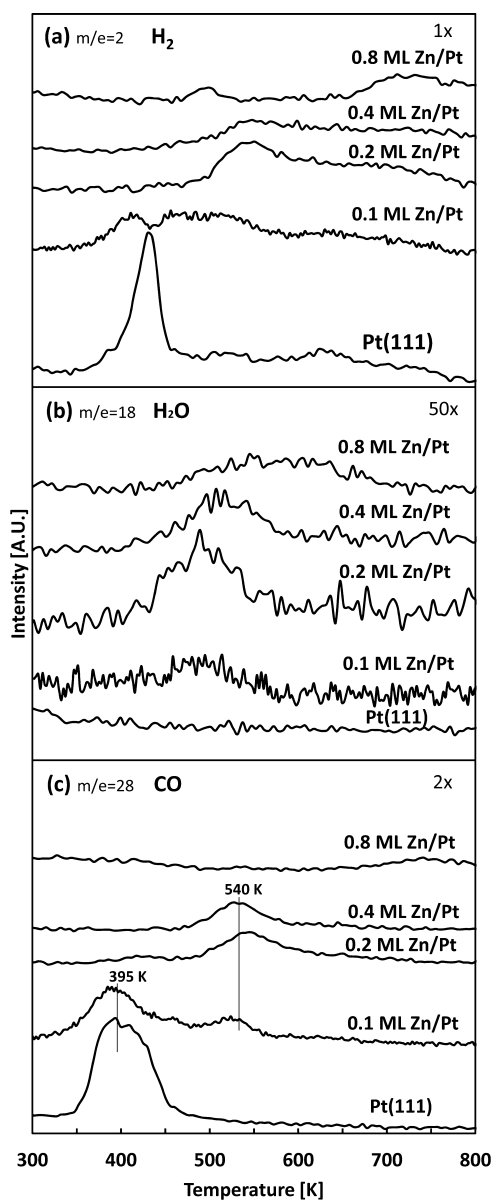


**Figure 3.** TPD spectra for (a)  $m/e$  2  $H_2$ , (b)  $m/e$  18  $H_2O$ , and (c)  $m/e$  28  $CO$  from  $Zn/Pt(111)$  as a function of Zn coverage. Each sample was dosed with 0.6 L of furfural at 115 K.

was a small amount of propene ( $m/e$  41), which desorbed at 365 K, indicating that both C–C and C–O bond cleavage in adsorbed furfural commences at or below this temperature. The TPD results for furfural on  $Pt(111)$  are similar to those reported previously for the reaction of acetaldehyde and glycolaldehyde on this surface.<sup>14</sup>

TPD data for the reaction of furfural on  $Pt(111)$  modified with 0.1, 0.4, and 0.8 ML of Zn adatoms are displayed in Figure 3. In each experiment, the sample, held at 115 K, was dosed with 0.6 L of furfural. The furfural TPD data for Zn-free  $Pt(111)$  are also included in the figure for comparison. These data show that adding Zn to the  $Pt(111)$  surface causes significant changes in the stability and reaction pathways for adsorbed furfural. As shown in Figure 1, which displays the TPD curves for desorption of molecular furfural, the parent molecule still desorbed in two overlapping peaks between 185 and 195 K, but the higher-temperature furfural peak at 225 K decreased in intensity with increasing Zn coverage and was not

observed for the 0.4 and 0.8 ML  $Zn/Pt(111)$  surfaces. The amount of molecular furfural desorbing from the Zn-modified surfaces was also significantly less than that from the Zn-free surface, suggesting that the Zn adatoms decrease the furfural sticking probability. More dramatic changes were observed for the  $H_2$  and  $CO$  products (Figure 3), which were produced at higher temperatures on the Zn-modified surfaces. Additionally, a small amount of  $H_2O$  and  $CO_2$  was also produced on the Zn-modified surfaces.

For 0.1 ML  $Zn/Pt(111)$ ,  $CO$  desorbed in two peaks centered at 400 and 525 K (Figure 3c). Upon increasing the Zn coverage to 0.4 ML, the 400 K  $CO$  peak disappeared, indicating that it corresponds to  $CO$  adsorbed on Zn-free portions of the surface. The  $CO$  peak at 525 K persisted for Zn coverages up to 0.4 ML but was absent from the 0.8 ML  $Zn/Pt(111)$ , the  $CO$  peak at 525 K was absent and the only  $CO$  features were two small peaks centered at 750 and 900 K.

As shown in Figure 3a, for all of the furfural-dosed surfaces  $H_2$  was produced in a series of overlapping peaks over a wide temperature range. The general trends in the  $H_2$  desorption data with increasing Zn adatom coverage include a rapid decrease in the intensity of the  $H_2$  peak at 450 K which dominated the spectrum for the Zn-free surface and a shift of the remaining  $H_2$  features to higher temperatures. For example, for 0.4 ML  $Zn/Pt(111)$ , the  $H_2$  desorption spectrum consists of a broad feature that spans between 500 and 800 K. Small amounts of  $H_2O$  (Figure 3b) and a trace amount of  $CO_2$  were also produced via reaction of furfural on the Zn-modified  $Pt(111)$  surfaces. For 0.1 ML  $Zn/Pt(111)$  a broad  $H_2O$  peak is evident at 520 K (Figure 3b). This peak increases in intensity and shifts to higher temperatures with increasing Zn coverage. The  $CO_2$  product (not shown in the figure) was only observed for the 0.4 and 0.8 ML Zn coverages and gave rise to a small peak between 500 and 675 K.

HREEL spectra collected as a function of temperature for Zn-free and 0.4 ML  $Zn/Pt(111)$  surfaces dosed with 0.6 L of furfural at 115 K are displayed in Figures 4 and 5, respectively. The spectra corresponding to surface temperatures higher than the dosing temperature were obtained by briefly heating the dosed sample to the indicated temperature and then rapidly quenching to 115 K, at which point the spectrum was collected. For the Zn-free  $Pt(111)$  surface, the HREEL spectrum obtained after dosing at 115 K (Figure 4) is consistent with the IR and Raman spectra of furfural<sup>20–22</sup> and the HREEL spectrum of molecular furfural adsorbed on  $Mo_2C/Mo(110)$  and  $Mo_2C/Mo(100)$  at low temperature.<sup>17,23</sup> Peak assignments for the spectrum of furfural on  $Pt(111)$  at 115 K were made by comparison to those reported for the aforementioned reference spectra and are reported in Table 1. Notable peaks in the spectrum include the  $\nu(C=O)$  stretch at  $1665\text{ cm}^{-1}$  and the  $\nu_{\text{ald}}(\text{CH})$  stretch at  $2790\text{ cm}^{-1}$ , both of which are indicative of the aldehyde functional group.

Heating the furfural-dosed  $Pt(111)$  surface to 155 K produced only minor changes in the intensities of the peaks in the HREEL spectrum. Further heating to 205 K, however, resulted in significant changes, including decreases in the intensities of the aldehyde  $\nu(C=O)$  stretch at  $1665\text{ cm}^{-1}$ , the ring breathing modes at  $1015$  and  $1565\text{ cm}^{-1}$ , and the  $\nu(C=C)$  stretch at  $1450\text{ cm}^{-1}$ . Large peaks at  $1805$  and  $2050\text{ cm}^{-1}$ , which are indicative of the  $\nu(C=O)$  mode of atop and bridging  $CO$  species on  $Pt(111)$ ,<sup>24</sup> also emerged, indicating that cleavage of the C–CHO bond in the adsorbed furfural has commenced by this temperature.

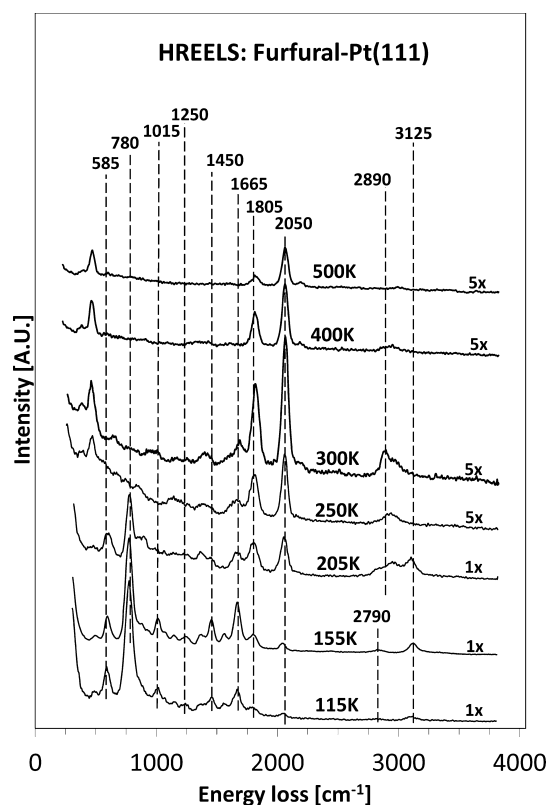


**Figure 4.** HREEL spectra as a function of temperature for a Pt(111) surface dosed with 0.6 L of furfural at 115 K.

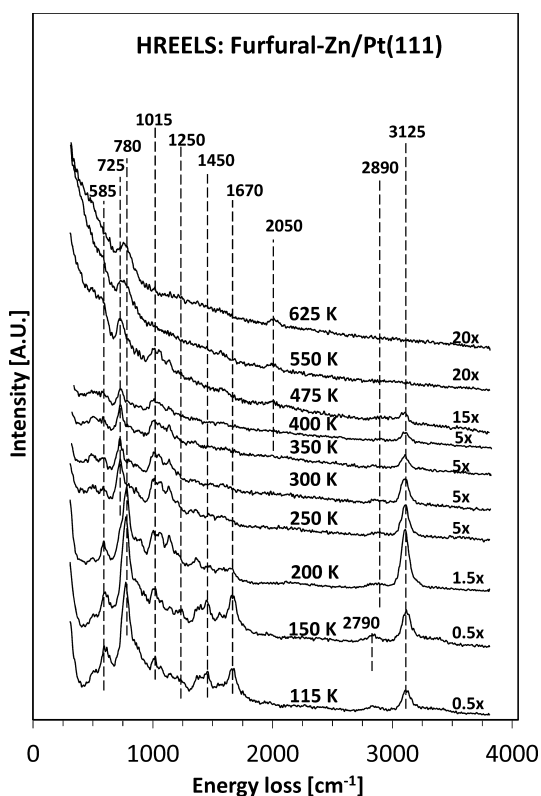


**Figure 5.** HREEL spectra as a function of temperature for a 0.4 ML Zn/Pt(111) surface dosed with 0.6 L of furfural at 115 K.

Heating to 250 K and then 300 K caused growth in the intensities of the  $\nu(\text{C}=\text{O})$  peaks of atop and bridging CO at

1805 and 2050  $\text{cm}^{-1}$  and the disappearance of the  $\nu_{\text{ring}}(\text{CH})$  peak at 3125  $\text{cm}^{-1}$  along with a concomitant increase in the intensities of several overlapping  $\nu(\text{CH})$  peaks between 2700 and 3000  $\text{cm}^{-1}$ . The changes in the C–H stretching region indicate a loss of the aromatic character of the remaining hydrocarbon species on the surface. This is further corroborated by the disappearance of the  $\gamma_{\text{ring}}(\text{OCC})$  (585  $\text{cm}^{-1}$ ) and  $\gamma_{\text{ring}}(\text{CH})$  (780  $\text{cm}^{-1}$ ) peaks upon heating to 300 K. Additional heating resulted in decomposition of the remaining hydrocarbon fragments on the surface, and the HREEL spectra contained only features indicative of atop and bridging CO.

HREEL spectra as a function of temperature for furfural-dosed, Zn-modified Pt(111) are displayed in Figure 5. For these studies a 0.4 ML Zn coverage was selected as a representative Zn adatom surface. The spectrum obtained after dosing 0.6 L of furfural at 115 K was nearly identical to that obtained from clean Pt(111) at the same temperature and was consistent the IR and Raman spectra of furfural.<sup>17,20–23</sup> Peak assignments are listed in Table 1. Notable features in the spectrum include the  $\gamma_{\text{s}}(\text{CH})$  and  $\gamma_{\text{as}}(\text{CH})$  peak at 780  $\text{cm}^{-1}$ , the  $\nu(\text{C}=\text{O})$  stretch at 1670  $\text{cm}^{-1}$ , and the  $\nu_{\text{ald}}(\text{CH})$  stretch at 2790  $\text{cm}^{-1}$ .

Heating to 200 K, which as shown in Figure 1 is sufficient to desorb any weakly adsorbed furfural, resulted in considerable alteration of the relative intensities of the peaks. The most noticeable was a dramatic decrease in the relative intensity of the  $\nu(\text{C}=\text{O})$  stretch, which also shifted slightly from 1670 to 1655  $\text{cm}^{-1}$ , and an increase in the intensity of the in-plane ring stretching modes between 900 and 1250  $\text{cm}^{-1}$ . A slight shift in position of the  $\nu_{\text{ald}}(\text{CH})$  mode of the aldehyde group from 2790 to 2890  $\text{cm}^{-1}$  also occurred upon heating to 200 K.

Heating from 200 to 250 K caused the  $\nu(\text{C}=\text{O})$  stretch of the aldehyde group at 1655  $\text{cm}^{-1}$  to a further decrease in intensity. As will be discussed below, the disappearance of this peak may be due to a shift from an  $\eta^1(\text{O})$  to an  $\eta^2(\text{C},\text{O})$  bonding configuration for the aldehyde carbonyl. Additional significant changes that occurred upon heating to 250 K include a downward shift in the position of the  $\gamma_{\text{s}}(\text{CH})$  and  $\gamma_{\text{as}}(\text{CH})$  wagging modes of the aromatic ring from 780 to 725  $\text{cm}^{-1}$  and a large decrease in the intensity of the  $\gamma_{\text{ring}}(\text{OCC})$  mode at 585  $\text{cm}^{-1}$ .

Except for a gradual decrease in the intensity of all of the peaks, heating from 250 to 400 K produced relatively few changes in the spectrum, with the only significant one being a slight downward shift in the position of the  $\nu(\text{CH})$  stretch near 3120  $\text{cm}^{-1}$ . This indicates that the adsorbed intermediates were relatively stable in this temperature range. It is notable that, in contrast to clean Pt(111), these HREELS data show that the aromatic ring of adsorbed furfural remains largely intact on the Zn-modified surface at temperatures up to 475 K. Further increasing the temperature to 550 K resulted in the decomposition of the surface intermediate to CO and H<sub>2</sub>, as evidenced by the emergence of a  $\nu(\text{C}=\text{O})$  stretch at 2050  $\text{cm}^{-1}$  indicative of atop CO and the near-disappearance of the peaks associated with the furan ring.

## DISCUSSION

It is useful to first consider the adsorption and reaction of furfural on the Zn-free Pt(111) surface. The TPD data (Figure 2) show that furfural undergoes unselective decomposition on this surface to produce primarily CO and H<sub>2</sub> and a trace amount of propene. Since the combined CO and propene products have a carbon to oxygen ratio much less than the 5:2

Table 1. Vibrational Mode Assignments

mode <sup>a</sup>	frequency, cm <sup>-1</sup>						
	IR/Raman <sup>20</sup>	Raman <sup>22</sup>	Raman <sup>21</sup>	Mo <sub>2</sub> C/Mo(110) <sup>23</sup>	Mo <sub>2</sub> C/Mo(100) <sup>17</sup>	Pt(111)	Zn/Pt(111)
$\nu_{\text{ring}}(\text{CH})$	3030–3160	3153		3091	3075	3125	3125
$\nu_{\text{aldehyde}}(\text{CH})$	2813–2858			2882	2800, 2875	2790	2790
$\nu(\text{C}=\text{O})$	1665–1695	1684	1665	1644	1650	1665	1670
ring breath	1572		1570		1570	1565	1560
$\nu(\text{C}=\text{C})$	1393–1479	1570, 1466		1536, 1427	1435	1450	1450
$\delta_{\text{t}}(\text{OCH})$		1370, 1157		1353, 1136	1350	1365	1360
$\rho(\text{CH}), \chi(\text{CH})$	755–885		1398, 1464, 1475		1350	1365	1360
$\rho_{\text{aldehyde}}(\text{CH})$			1366				
$\rho_{\text{as}}(\text{CH}), \chi_{\text{as}}(\text{CH})$			1227	1238	1205	1250	1250
$\nu_{\text{ring}}(\text{CO})$		1025, 930	1156	1028	1125	1145	1145
ring breath			1078		1055	1015	1015
$\chi_{\text{s}}(\text{CH})$		950	1078, 1021		997		
$\gamma_{\text{aldehyde}}(\text{CH})$			951				
ring breath	500–630		932	866	865		
$\gamma_{\text{s}}(\text{CH}), \gamma_{\text{as}}(\text{CH})$ (ring)			761, 884	758	750	780	780
$\gamma_{\text{ring}}(\text{OCC})$			595		580	585	585
$\nu(\text{CC})$ (ring aldehyde)			508		500	495	500

<sup>a</sup>Abbreviations: s, symmetric; as, asymmetric; b, bend;  $\nu$ , stretch;  $\delta$ , deformation;  $\rho$ , rock;  $\gamma$ , wag;  $\chi$ , scissor.

ratio in the furfural reactant, some carbon must have been deposited on the surface. The HREELS results in conjunction with data from the literature provide insight into the intermediates involved in this unselective decomposition pathway. Previous studies have shown that the most stable adsorption geometry for furan on Pt(111) is with the planar aromatic ring lying parallel to the surface.<sup>25</sup> Small aldehydes are also known to undergo C–H cleavage in the aldehyde group at temperatures below 200 K on this surface to form acyl intermediates<sup>14,26</sup> which are susceptible to decarbonylation upon heating. For furfural, both of these bonding modes need to be considered.

The HREEL spectrum of the furfural-dosed surface at and below 205 K is dominated by the peak at 780 cm<sup>-1</sup>, which is due to the out-of-plane C–H wagging modes of the furan ring. In contrast, the in-plane  $\nu_{\text{ring}}(\text{CO})$  and ring breathing modes between 1000 and 1200 cm<sup>-1</sup> are of much lower intensity. These relative intensities differ from that in the IR spectrum of gaseous furfural, where the in-plane and out-of-plane ring modes have similar cross sections.<sup>20</sup> Sum frequency generation vibrational spectroscopy studies by Kliewer et al.<sup>25</sup> have shown that furan adsorbs on Pt(111) with the ring parallel to the surface. Assuming a similar bonding configuration for furfural on Pt(111), the dipole moments associated with the in-plane modes would be largely shielded by the induced image dipoles in the metal, resulting in low adsorption cross sections, which is consistent with the HREELS data reported here.

The HREELS data in Figure 4 also do not provide any evidence for strong interaction of the aldehyde carbonyl in furfural with the Pt(111) surface. Note that below 250 K the spectrum of the furfural-dosed surface contains a  $\nu_{\text{ald}}(\text{C}=\text{O})$  peak at 1665 cm<sup>-1</sup> which is essentially at the same position as that in the IR spectrum of the free molecule.<sup>20</sup> This peak would be expected to be nearly absent (due to the surface dipole selection rules) and shift significantly to lower wavenumbers if the aldehyde group was in an  $\eta^2(\text{C},\text{O})$  configuration in which both the C and O are bonded to the surface.<sup>14,17</sup> Formation of an acyl intermediate via cleavage of the aldehyde C–H would also cause a shift to lower wavenumbers.<sup>14</sup> Acyl formation at temperatures below 250 K can also be ruled out by the

presence of the C–H stretching peak at 2790 cm<sup>-1</sup>, which is characteristic of the aldehyde C–H bond.

The HREELS data, therefore, show that furfural adsorbs on Pt(111) with the furan ring situated either parallel or nearly parallel to the surface and that the aldehyde carbonyl does not interact strongly with the surface. Thus, the surface bonding appears to occur via the  $\pi$  orbitals in the ring. This conclusion is consistent with a recent study by Liu et al.<sup>27</sup> in which DFT calculations indicated that the most stable adsorption geometry for furfural on Pt(111) was with the aromatic ring centered on a 3-fold hollow site and the aldehyde group tilted away from the surface. They also concluded that the largest bonding contribution was due to interaction of the unsaturated C=C bonds in the ring with the surface. It is noteworthy that this result is somewhat different than what they<sup>27</sup> and others<sup>28</sup> have obtained by DFT for the adsorption of furfural on Pd(111), where both the aromatic ring and the aldehyde carbonyl are parallel to the surface in the most stable adsorption geometry.

The HREELS data in Figure 4 also show that C–C bond scission and ring opening in adsorbed furfural on Pt(111) commences by 205 K. This is evident by the appearance of  $\nu(\text{CO})$  peaks for bridging (1805 cm<sup>-1</sup>) and atop (2050 cm<sup>-1</sup>) CO and a new, distinct  $\nu(\text{C–H})$  peak at 2890 cm<sup>-1</sup> which is characteristic of aliphatic CH<sub>x</sub> groups on the surface. Ring opening is also demonstrated by the production of a small amount of propene at 365 K during TPD. Above 300 K decomposition of the furfural is nearly complete, with adsorbed CO and small hydrocarbon fragments being the primary surface species.

The TPD results show that furfural is significantly more stable on the Zn-modified Pt(111) surfaces with reaction-limited decomposition products desorbing at temperatures above 450 K. This stability is also reflected in the HREELS data obtained from the 0.4 ML Zn/Pt(111) surface. At 200 K, the HREEL spectrum is consistent with the IR spectrum of molecular furfural (see Table 1),<sup>20</sup> and in contrast to the corresponding data from Zn-free Pt(111), the relative intensities of the in-plane and out-of-plane ring modes suggest that the furan ring is not situated parallel to the surface. The large decrease in the relative intensity of the  $\nu(\text{C}=\text{O})$  peak

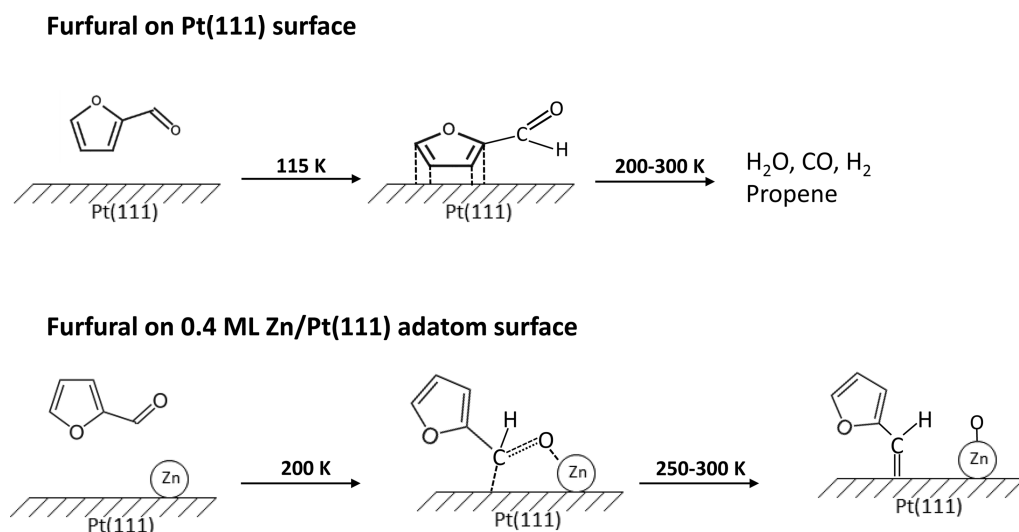


**Figure 6.** Proposed pathways and intermediates for the adsorption and reaction of furfural on Pt(111) and Zn/Pt(111) surfaces.

upon heating from 150 to 250 K is consistent with the carbonyl of the aldehyde group being in an  $\eta^2(\text{C},\text{O})$  configuration in which both the C and O are bonded to the surface<sup>9</sup> and with what has been reported previously for both acetaldehyde and glycolaldehyde on Zn-modified Pt(111).<sup>14</sup> In these previous studies it was concluded on the basis of XPS data that the O atom in the aldehyde carbonyl is bonded to a Zn site and the C is bonded to Pt. We, therefore, conclude that there is a similar bonding configuration for the aldehyde group in furfural on Zn-modified Pt(111) surfaces at low temperatures. This bonding configuration is shown schematically in Figure 6.

Changes in the structure and/or bonding of the adsorbed furfural are apparent upon heating from 200 to 250 K. The HREELS data show little alteration in the peaks associated with the aromatic ring between 800 and 1450  $\text{cm}^{-1}$  as well as the furan ring C–H stretch at 3125  $\text{cm}^{-1}$ , thus indicating that the furan ring remains intact. There are, however, two significant changes in the spectrum: a shift of the lower energy  $\nu(\text{CH})$  peak from 2790 to 2890  $\text{cm}^{-1}$  and a shift of the intense peak at 780  $\text{cm}^{-1}$  due to the ring  $\gamma_s(\text{CH})$  and  $\gamma_{as}(\text{CH})$  modes to 725  $\text{cm}^{-1}$ . The shift in the position of the  $\nu(\text{CH})$  peak is significant because it indicates some alteration in the bonding or structure of the –CHO group. It is possible that this shift may be related to the formation of an  $\eta^2(\text{C},\text{O})$  intermediate. It is also noteworthy that this C–H stretch, which is distinct from that associated with the furan ring (3125  $\text{cm}^{-1}$ ), is apparent for temperatures up to 475 K, since this argues against cleavage of the C–H bond in the –CHO group and the formation of an acyl intermediate. Note that this conclusion is consistent with what has been reported previously for acetaldehyde and glycolaldehyde, where the addition of Zn to the Pt(111) was also found to hinder acyl formation which is facile on the Zn-free surface.<sup>14</sup>

The shift in the  $\gamma_s(\text{CH}) + \gamma_{as}(\text{CH})$  peak to lower wavenumbers is more difficult to explain. The HREELS data do not provide any evidence for a strong interaction of the furan ring with the surface, since these are the only ring-related modes that are altered. In our previous studies of the reaction of acetaldehyde and glycolaldehyde on Zn-modified Pt(111) it was concluded on the basis of HREELS data that the  $\eta^2(\text{C},\text{O})$ -bonded carbonyl group in these molecules undergoes C–O bond cleavage near room temperature. A similar reaction would

therefore be expected for the  $\eta^2(\text{C},\text{O})$ -bonded furfural on this surface. By this scenario the shifts in both the  $\nu_{\text{ald}}(\text{CH})$  and  $\gamma_{\text{ring}}(\text{CH})$  modes could result from this C–O bond cleavage reaction. The IR spectra of substituted furans provide some support for this. Note that, in the IR spectra of furfural, 2-furfuryl alcohol, and 2-methylfuran the  $\gamma_{\text{ring}}(\text{CH})$  mode is located at 754, 735, and 722  $\text{cm}^{-1}$ ,<sup>20,29</sup> respectively, indicating that removal of the electron-withdrawing oxygen in the substituent group causes the  $\gamma_{\text{ring}}(\text{CH})$  modes to shift to lower wavenumbers. The production of a small amount of water between 400 and 600 K during TPD of furfural-dosed Zn-modified Pt(111) surfaces (see Figure 3b) also provides some support for C–O cleavage in the adsorbed intermediate.

On the basis of the TPD data and the analysis of the HREEL spectra, we propose the reaction pathways and intermediates shown schematically in Figure 6 for the reaction of furfural on Zn-modified Pt(111) surfaces. At low temperatures (<250 K), furfural interacts with the surface primarily via the aldehyde carbonyl with the aromatic furan ring tilted away from the surface. At 200 K this carbonyl bonds to the surface in an  $\eta^2(\text{C},\text{O})$  configuration. By analogy to results reported in previous studies for acetaldehyde and glycolaldehyde on Zn-modified Pt(111),<sup>14</sup> it is assumed that the oxygen in the carbonyl is bonded to a Zn site and the carbon is bonded to a Pt site. The bonding to the surface for this intermediate occurs via electron donation from the metal d orbitals into the unoccupied  $\pi^*$  antibonding orbitals of the carbonyl. This causes a reduction in the strength of the C–O bond, which helps facilitate its cleavage that occurs between 250 and 300 K. As shown in Figure 6, this produces a  $(\text{C}_4\text{H}_3\text{O})\text{--CH=}$  intermediate. This intermediate is relatively stable, since it remains intact up to 400 K (as determined by HREELS). Recall that on the pristine Pt surface furfural decomposed completely and unselectively below 300 K. The thermal stability of the  $(\text{C}_4\text{H}_3\text{O})\text{--CH=}$  intermediate on the Zn-modified surface therefore further demonstrates that the addition of Zn to Pt decreases the metal's activity for C–C and C–H bond cleavage.

Under typical HDO reaction conditions where there would be a high coverage of H atoms on the catalyst, one would anticipate that the  $(\text{C}_4\text{H}_3\text{O})\text{--CH=}$  intermediate could be hydrogenated to produce 2-methylfuran. Thus, the results of this study suggest that PtZn may exhibit high selectivity for the

HDO of furfural to produce 2-methylfuran. The results of this study also provide insight into why addition of an oxyphilic metal, such as Zn, to group 10 metals enhances activity for selective HDO of aromatic oxygenates without hydrogenation of the aromatic ring. The key observation obtained here is that the Zn significantly weakens the interaction of the furan ring with the Pt surface, producing intermediates in which the ring is tilted away from the surface, thereby preventing its hydrogenation.

## CONCLUSIONS

This study provides insight into the adsorption and reaction of the biomass-derived oxygenate, furfural, on Pt(111) and Zn-modified Pt(111) surfaces. For Zn-free Pt(111), furfural primarily interacts with the surface via the aromatic ring and undergoes C–C bond scission and ring opening at temperatures as low as 200 K, which leads to unselective decomposition to CO and H<sub>2</sub> at higher temperatures. Modifying the Pt(111) surface with Zn adatoms significantly alters the bonding of furfural with an  $\eta^2(\text{C},\text{O})$  configuration in which the furan ring is tilted away from the surface being the most stable at 200 K. This bonding configuration results in a weakening of the carbonyl C–O bond, facilitating its cleavage. The lack of a strong interaction of the aromatic furan ring with the Zn-modified surface would also be expected to help limit hydrogenation of the ring under typical HDO reaction conditions. These results suggest that PtZn catalysts may have high activity for the selective HDO of furfural to produce methylfuran.

## AUTHOR INFORMATION

### Corresponding Author

\*J.M.V.: e-mail, [Vohs@seas.upenn.edu](mailto:Vohs@seas.upenn.edu); tel, 1-215-898-6318.

### Notes

The authors declare no competing financial interest.

## ACKNOWLEDGMENTS

Funding for this study was provided by the U.S. Department of Energy, Office of Science, Office of Basic Energy Sciences, under Grant No. DE-FG02-04ER15605.

## REFERENCES

- (1) Huber, G. W.; Iborra, S.; Corma, A. *Chem. Rev.* **2006**, *106* (9), 4044–4098.
- (2) Gallezot, P. *Chem. Soc. Rev.* **2012**, *41* (4), 1538–1558.
- (3) Stöcker, M. *Angew. Chem., Int. Ed.* **2008**, *47* (48), 9200–9211.
- (4) Alonso, D. M.; Bond, J. Q.; Dumesic, J. A. *Green Chem.* **2010**, *12* (9), 1493–1513.
- (5) Li, H.; Luo, H.; Zhuang, L.; Dai, W.; Qiao, M. *J. Mol. Catal. A: Chem.* **2003**, *203* (1), 267–275.
- (6) Liaw, B.-J.; Chiang, S.-J.; Chen, S.-W.; Chen, Y.-Z. *Appl. Catal., A* **2008**, *346* (1), 179–188.
- (7) Sitthisa, S.; Resasco, D. E. *Catal. Lett.* **2011**, *141* (6), 784–791.
- (8) Reddy, B. M.; Reddy, G. K.; Rao, K. N.; Khan, A.; Ganesh, I. *J. Mol. Catal. A: Chem.* **2007**, *265* (1), 276–282.
- (9) Sitthisa, S.; An, W.; Resasco, D. E. *Catal. Lett.* **2011**, *284* (1), 90–101.
- (10) Yu, W.; Xiong, K.; Ji, N.; Porosoff, M. D.; Chen, J. G. *Catal. Lett.* **2014**, *317*, 253–262.
- (11) Nakagawa, Y.; Nakazawa, H.; Watanabe, H.; Tomishige, K. *ChemCatChem* **2012**, *4* (11), 1791–1797.
- (12) González-Borja, M. Á.; Resasco, D. E. *Energy Fuels* **2011**, *25* (9), 4155–4162.
- (13) Parsell, T. H.; Owen, B. C.; Klein, I.; Jarrell, T. M.; Marcum, C. L.; Hauptert, L. J.; Amundson, L. M.; Kenttämää, H. I.; Ribeiro, F.; Miller, J. T. *Chem. Sci.* **2013**, *4* (2), 806–813.
- (14) McManus, J. R.; Martono, E.; Vohs, J. M. *ACS Catal.* **2013**, *3* (8), 1739–1750.
- (15) McManus, J. R.; Vohs, J. M. *Appl. Surf. Sci.* **2013**, *271*, 45–51.
- (16) McManus, J. R.; Salciccioli, M.; Yu, W.; Vlachos, D. G.; Chen, J. G.; Vohs, J. M. *J. Phys. Chem. C* **2012**, *116* (35), 18891–18898.
- (17) McManus, J. R.; Vohs, J. M. *Surf. Sci.* **2014**.
- (18) Koel, B.; Roszell, J.; Martono, E.; Vohs, J. In *Low-energy Alkali Ion Scattering and X-ray Photoelectron Diffraction Studies of the Structure of Pt-Zn/Pt (111) Bimetallic Surfaces*; APS Meeting Abstracts, 2013; p 40015.
- (19) Seebauer, E.; Kong, A.; Schmidt, L. *Surf. Sci.* **1986**, *176* (1), 134–156.
- (20) Allen, G.; Bernstein, H. *Can. J. Chem.* **1955**, *33* (6), 1055–1061.
- (21) Jia, T.-j.; Li, P.-w.; Shang, Z.-g.; Zhang, L.; He, T.-c.; Mo, Y.-j. *J. Mol. Struct.* **2008**, *873* (1), 1–4.
- (22) Kim, T.; Assary, R. S.; Curtiss, L. A.; Marshall, C. L.; Stair, P. C. *J. Raman Spectrosc.* **2011**, *42* (12), 2069–2076.
- (23) Xiong, K.; Lee, W. S.; Bhan, A.; Chen, J. G. *ChemSusChem* **2014**.
- (24) Baro, A.; Ibach, H. *J. Chem. Phys.* **1979**, *71* (12), 4812–4816.
- (25) Kliewer, C. J.; Aliaga, C.; Bieri, M.; Huang, W.; Tsung, C.-K.; Wood, J. B.; Komvopoulos, K.; Somorjai, G. A. *J. Am. Chem. Soc.* **2010**, *132* (37), 13088–13095.
- (26) Zhao, H.; Kim, J.; Koel, B. E. *Surf. Sci.* **2003**, *538* (3), 147–159.
- (27) Liu, B.; Cheng, L.; Curtiss, L.; Greeley, J. *Surf. Sci.* **2014**, *622*, 51–59.
- (28) Pang, S. H.; Medlin, J. W. *ACS Catal.* **2011**, *1* (10), 1272–1283.
- (29) *NIST Chemistry WebBook, NIST Standard Reference Database*; Linstrom, P. J., Mallard, W. G., Eds.; National Institute of Standards and Technology: Gaithersburg, MD 20899; No. 69, <http://webbook.nist.gov>.